Progress In Electromagnetics Research B, Vol. 22, 321–340, 2010

NEW FORMULATION OF THE ITERATIVE METHOD: APPLICATION TO A MICROWAVES ATTENUATOR

F. Mejri and T. Aguili

Syscom Laboratory
Engineers' National School of Tunis
B.P. 37 Le belvedere 1002, Tunis, Tunisia

H. Baudrand

E.N.S.E.E.H.T, 2 rue Ch Camichel B.P. 7122
Toulouse Cdx7 31071, France

Abstract—In this article, we developed a new method of calculation of the active microwaves circuits in micro ribbon technology. This technique is based on the iterative method where localised auxiliary sources are introduced to model the active elements of the circuit (ultra high frequency diodes). To validate this work, the results obtained are compared with those obtained by the software momentum of advanced design system (ADS). We show primarily the interests and the operational limits of auxiliary source in the formulation of the considered problem.

1. INTRODUCTION

Nowadays, the interest is carried more and more to the active planar microwaves circuits, in particular for their applications in telecommunications. The last ones carried out on substrate of silicon, are often used in mobile telephony for intermediate frequency. The use of substrate of alumina and gallium arsenide are being particularly and respectively reserved for the hybrid circuits and various functions in millimetre-length waves. The active parts are characterized by very small dimensions — of the order of the micron — in respect of the waves' length and both the transverse and longitudinal dimensions of the lines forming the circuit. This multi-scale character raised serious problems to the originators: indeed, to describe the totality of the circuit with a fine grid — necessarily imposed by the active element

Corresponding author: F. Mejri (fethi_mejri@laposte.net).

— makes the resolution of the problem with traditional methods "full waves" almost impossible (the numerical criterion of stability in method finite difference temporal domain (FDTD) is generally limited by the length of debye of the semiconductor). To circumvent this difficulty, several authors considered a variable grid in the same software which by a very tight grid would describe details of multiple heterogeneities of a located element. Then with a looser grid, it would take into account the lines of excitations and the case. But very quickly, we realize that this manner of proceeding is more difficult to implement: indeed the setting in equation of the variable grid and the filling of the matrices considered in calculation are not automatic any more.

To avoid these useless steps consisting in simulating low-size elements, a solution resides in the introduction of the localised elements "lumped element" [1] into the electromagnetic software: finite elements [2], finished differences [3]. Another more rigorous solution consists in simulating the various parts of the circuit by adequate methods and equalizing the fields in extreme cases of the fields [4]. However, the introduction of these elements considered without dimensions can cause divergences in the results according to the precision of the grid, whereas the electromagnetic properties of the circuits must be independent of the adapted grid. Indeed the coupling between the distributed elements (environment or external parts) and the active elements (located or interior) must be done independently of the grid or the selected numerical method. This can be carried out in electromagnetism by applying the principle of Huygens or of equivalence which consists in formulating easily the equivalent problem by replacing the current sources by equivalent or fictitious sources producing the same electromagnetic field in the considered area. An electric field on an open guide can be replaced by two opposite magnetic power sources. However, the application of this principle to the located elements without dimensions is not possible under penalty of divergence of the computation results. To avoid this approach of the active element (or localised) by passage in extreme cases of null size, we consider an equivalence between elements by the identity of their electric characteristics. Indeed, the study of the reaction of the active element in a circuit requires neither the knowledge of manufacture technology nor the detailed description of the working procedure of this element, only their electric characteristics will be considered. Therefore the passage of an electromagnetic description of the circuit to an electric description of the active element is carried out easily by the introduction of sources which one calls "auxiliary sources". These sources are used as intermediate calculation and translate naturally the principle of equivalence. However, two difficulties emerge:

- Exact modelling of the real environment of the active element.
- Passage of the formalism of Maxwell to that of Kirchhoff (description of the active element).

On the one hand, to avoid any representation in multi port of the active element, we consider that all the evanescent modes intervening in calculation are considered completely attenuated in the vicinity of this element. In addition, the equivalence between electric field/magnetic field and tension/current is ensured by low-size surfaces (quasi-static assumption) covered with magnetic walls.

To illustrate these phenomena, in this work, we will focus on the study of a microwaves attenuator represented on Figure 1. Its functioning is based on a network in $\prod$ with diodes PIN. The attenuation function can be met in emission as in reception. It is also used in the amplifiers with automatic ordering of profit.

In this work, we only consider the high frequency part (HF) of the attenuator, which is represented in gray on Figure 1. It consists of

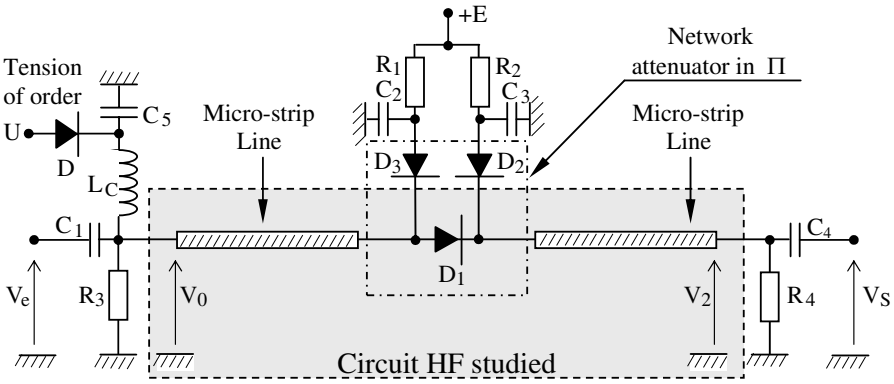

Figure 1. General diagram of a microwaves attenuator.

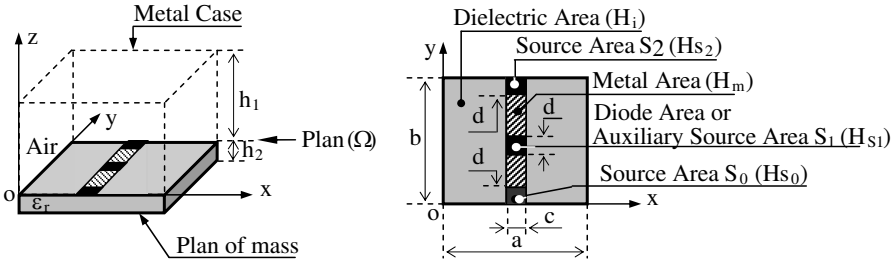

Figure 2. Structure of study and plan of discontinuity Ω.

a diode D_1 inserted between two micro strip lines of characteristic impedances Z_C and two sources of localised fields $S_0\{E_0, J_0\}$ and $S_2\{E_2, J_2\}$ representing respectively the tensions V_0 and V_2 into the entry and the exit of the attenuator. This circuit is located at the interface Ω between two dielectric mediums, of relative permittivity ε_{r1} and ε_{r2} supposed without losses (see Figure 2).

2. FORMULATION OF THE PROBLEM

At the beginning, we present the electromagnetic model of the structure to be studied as well as the technique of the auxiliary source. In continuation, we apply the method of analysis to this structure to extract the results from the problem in order to validate them.

2.1. Electromagnetic Model of the Studied Structure

For reasons of shielding and modeling, the studied circuit will be placed in a cavity with metal walls as shown in Figure 2.

Structural parameters: $a = 12\,\text{mm}$, $b = 20.4\,\text{mm}$, $c = 0.75\,\text{mm}$, $d = 1.275\,\text{mm}$, $h_1 = 1.62\,\text{mm}$, $h_2 = 0.38\,\text{mm}$, $\varepsilon_r = 9.7$.

Characteristics of the diode: $R_p = 1\,\Omega$, $R_n = 1\,\Omega$, $R_i =$ Variable, $C = 0.1\,\text{pF}$.

- In direct polarization: R_i evolve of $10\,\text{k}\Omega$ for $1\,\mu\text{A}$ to $1\,\Omega$ for $1\,\text{A}$.
- In opposite polarization: R_i superior with $10\,\text{k}\Omega$.

The used diode is a diode PIN. In mode of direct polarization, it has a variable resistor whose value is inversely proportional to current I_d.

$$R_I = K \cdot (I_d)^{-x} \tag{1}$$

With: $x \cong 0.9$ and K: proportionality factor.

The admittance Y_d obtained starting from its equivalent electric diagram is:

$$Y_d = jC\omega + (1/(R_p + R_i + R_n)) \tag{2}$$

2.2. Technique of the Auxiliary Source

To avoid a total modelling of a planar structure integrating an active component (diode, transistor), we employ the technique of the auxiliary sources which consists in breaking up the active circuit into two parts (see Figure 3):

- distributed passive elements (P)
- localised active elements (A).

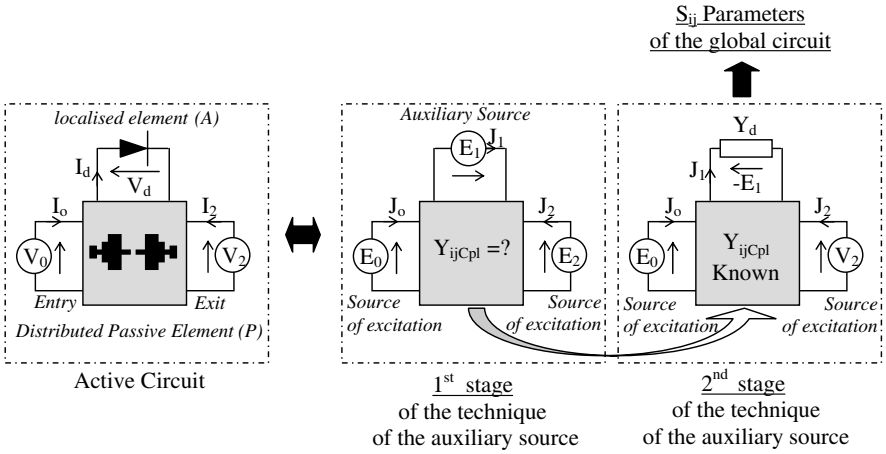

Figure 3. Auxiliary source technique.

This makes it possible to divide the study into two parts. We start with an electromagnetic analysis of the passive element of the circuit, by replacing the diode by a localised auxiliary source. We calculate in this first stage all the elements Y_{ij} of the coupling matrix between the various sources of the structure. Then we place between the electrodes anode-cathode, a localised access allowing the connection of the equivalent diagram of the diode. We calculate in this second stage the parameters S_{ij} of the device. Thus the total structure of the circuit is modelled by holding account of all the electromagnetic interactions between the various parts of the circuit.

Therefore, it would be easier to calculate (P) independently of (A), then to connect them for the calculation of the unit.

The accuracy of the obtained results depends closely on the method with which we determine the intrinsic equivalent diagram of the diode, which is generally deduced by practical measurements.

2.3. Application of the Iterative Method with Auxiliary Source to the Structure of Study

The iterative method was developed in various theses and multiple articles [5–8], it is based on two types of waves, incidental (A_k) and reflected (B_k), respectively expressed in the space and modal fields, by the relations (6) and (7). The passage of these waves from one field to another is ensured by the iterative process using the fast modal transform (FMT), which is not other than the FFT balanced on each mode. The use of the FMT, reduces the computing time and

accelerates the convergence of the method, but requires description in pixels of the interface Ω. In any point of this interface a vector of wave associated with the electromagnetic field is defined $(\vec{E}, \vec{H})$ by:

$$A_k = \frac{1}{2\sqrt{z_{0k}}} (E_k + Z_{0k} \cdot J_k) \tag{3}$$

$$B_k = \frac{1}{2\sqrt{z_{0k}}} (E_k - Z_{0k} \cdot J_k) \tag{4}$$

in which, the density of current J_k is defined by the relation:

$$\vec{J_k} = \vec{H}_k \Lambda \vec{n}_k, \tag{5}$$

where k indicates the index of medium 1 or 2 separated by plan Ω; n_k is a normal vector with Ω; Z_{0k} is the impedance characteristic of the medium k and $(\vec{E}, \vec{H})$ are the tangential components of the electromagnetic field.

We can thus define an operator of diffraction $\hat{\Gamma}_\Omega$, giving the incidental waves starting from the reflected waves in the space field (which describes the image of the circuit to analyze) and a reflexion operator $\hat{\Gamma}_k$ giving the reflected waves starting from the incidental waves in the modal field (which describes the nature of the walls of the case and the dielectric one of the various mediums of the structure). The incidental and reflected waves are thus bound by the following relations:

$$\begin{cases} A_k^n = \hat{\Gamma}_\Omega B_k^n + A_k^0 & : \text{ Space field} \quad (6) \\ B_k^n = \hat{\Gamma}_k A_k^{n-1} & : \text{ Spectral field} \quad (7) \end{cases}$$

We find in appendix more details concerning these two relations.

For the functional analysis of the iterative process, we will consider that with initialization, the structure is excited by a source (level) which emits an incidental wave A_k^0 on both sides of the plan Ω. This wave is as well reflected by the higher half than by the lower half of the case to give rise to B_k^1 who will constitute the reflected waves of the first iteration. These waves are diffracted within discontinuity plan, by giving rise to incidental waves noted A_k^1, which in their turn will be reflected by both the lower and higher halves of the case, to give then rise to reflected waves of the second iteration noted B_k^2 and so on until n iteration where we reach the convergence of the results. At this time, we can calculate the parameters of the analyzed circuit.

Many works were undertaken with this approach to study simple or multi-layer planar circuits of arbitrary and even complex form, comprising only passive elements. But no study was undertaken on planar circuits including active elements (diodes, transistors). For that,

several efforts remain to be agreed on this subject, from which comes to be introduced our research task, which requires a new setting in equation of this iterative method by using the technique of the auxiliary sources to model the active elements of the studied circuit.

The integration of this technique in the iterative method consists in replacing initially the diode by a localised source of field. This makes the task easy to us to determine the electromagnetic coupling between the various sources of the circuit, activating them one after the other. Once this operation is finished, we connect the diode in its place in the circuit. After that we calculate the parameters of the total circuit from the results found in the first stage.

In this method, we notice the superiority of the use of the auxiliary sources by the simplicity of the formulation of the problem and by reducing the electromagnetic calculation of the passive element of the studied circuit, which is made only once for various parameters of the used diode or various types of diodes, knowing that this analysis requires much computing time.

The flow chart of Figure 4 summarizes this technique of work.

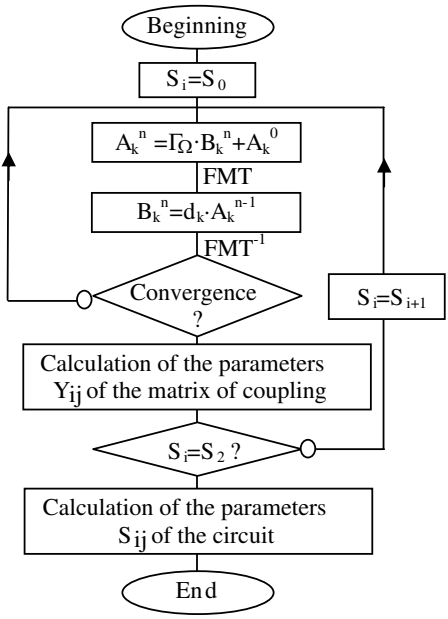

Figure 4. Flow chart summarizing the iterative method with auxiliary sources.

2.3.1. Electromagnetic Analysis of the Passive Element of the Studied Circuit (1st Stage)

In this first stage, we replace the diode by a localised auxiliary source, allowing the electromagnetic calculation of the equivalent hexa-pole seen from the three sources considered in Figure 2.

The structure of study of Figure 2 contains three localised sources. $S_0(E_0, J_0)$ and $S_2(E_2, J_2)$ respectively representing the signal at the entry and the exit of the attenuator. $S_1(E_1, J_1)$ models the P.I.N. diode. This makes it possible to establish the matrix of coupling (M) between these three sources.

$$\begin{pmatrix} J_0 \\ J_1 \\ J_2 \end{pmatrix} = \underbrace{\begin{pmatrix} Y_{11Cpl} & Y_{12Cpl} & Y_{13Cpl} \\ Y_{21Cpl} & Y_{22Cpl} & Y_{23Cpl} \\ Y_{31Cpl} & Y_{32Cpl} & Y_{33Cpl} \end{pmatrix}}_{(M)} \cdot \begin{pmatrix} E_0 \\ E_1 \\ E_2 \end{pmatrix} \tag{8}$$

The calculation of the elements Y_{ijCpl} of the matrix of coupling between the various sources of the circuit, is done by considering that the structure is alternatively excited by: $S_0(E_0, J_0)$ or by $S_1(E_1, J_1)$ or by $S_2(E_2, J_2)$.

(i) Case Where the Source $S_0(E_0, J_0)$ is Activated:

In this first case, sources $\{S_1$ and $S_2\}$ are short-circuited $(E_1 = E_2 = 0)$ thus the equations deduced from the matrix relation (8) result in:

$$Y_{11Cpl} = (J_0/E_0),\ Y_{21Cpl} = (J_1/E_0),\ Y_{31Cpl} = (J_2/E_0) \tag{9}$$

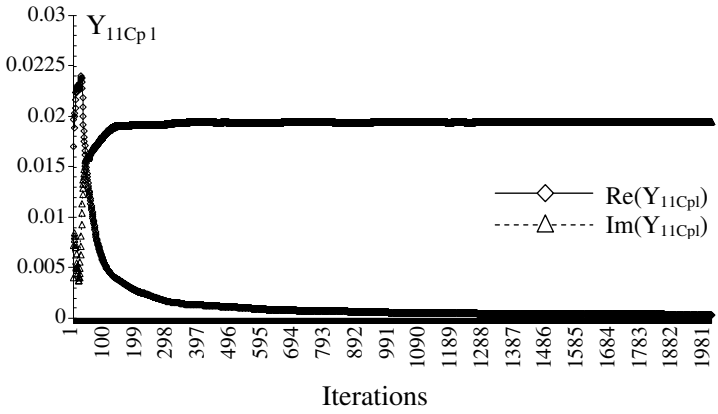

Figure 5. Convergence of the element Y_{11Cpl} according to the iterations (for $f = 5\,\mathrm{GHz}$).

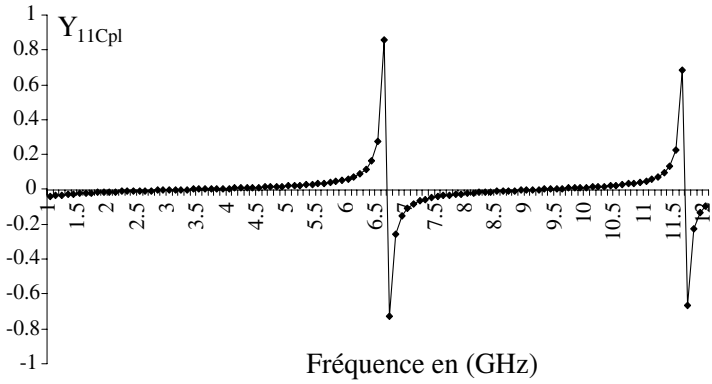

Figure 6. Variation of element Y_{11Cpl} according to the frequency.

J_0, J_1 and J_2 are the densities of current created by the source $\{S_0\}$ respectively on the level of the source itself and the site of the short-circuited sources $\{S_1$ and $S_2\}$. So that the parameters Y_{11Cpl}, Y_{21Cpl} and Y_{31Cpl} are respectively the admittance seen from the source of excitation $\{S_0\}$ and the admittances seen of the points occupied by the short-circuited sources $\{S_1$ and $S_2\}$.

In this analysis, we pass by a convergence study of the elements Y_{ijCpl} of the matrix of coupling according to the iterations, in order to optimize the computing time and to improve the precision of the results. We present at Figure 5 only the convergence of the element Y_{11Cpl}, which seems to be reached at the end of 500 iterations, for a frequency $f = 5\,\text{GHz}$ (Figure 5). The variation of the element Y_{11Cpl} according to the frequency is represented on Figure 6.

(ii) Case Where the Source $S_1(E_1, J_1)$ Is Activated

In this second case, sources $\{S_0$ and $S_2\}$ are short-circuited ($E_0 = E_2 = 0$) so the equations deduced from the matrix relation (8) result in:

$$Y_{12Cpl} = (J_0/E_1),\ Y_{22Cpl} = (J_1/E_1),\ Y_{32Cpl} = (J_2/E_1) \tag{10}$$

(iii) Case Where the Source $S_2(E_2, J_2)$ Is Activated

In this last case, sources $\{S_0$ and $S_1\}$ are short-circuited ($E_0 = E_1 = 0$), thus the equations deduced from the matrix relation (8) result in:

$$Y_{13Cpl} = (J_0/E_2),\ Y_{23Cpl} = (J_1/E_2),\ Y_{33Cpl} = (J_2/E_2) \tag{11}$$

Once the parameters Y_{ijCpl} of the coupling matrix have been calculated, we connect the diode at the boundaries of the equivalent hexa-pole seen from the three sources of the structure and we calculate the parameters S_{ij} of the attenuator. This work is the subject of the second stage of the technique of the auxiliary sources and which constitutes a total analysis of the studied circuit.

2.3.2. Total Analysis of the Studied Circuit (2nd Stage)

The modelling of a diode by a localised auxiliary source, leads us to the relation (12).

On the region of the diode we have:

$$\begin{array}{l} V_d = E_d \cdot d_1 \text{ and } I_d = J_d \cdot c \Rightarrow Y_d = (I_d/V_d) = (c/d_1) \cdot (J_d/E_d) \\ V_1 = -V_d \text{ and } J_1 = J_d \quad \Rightarrow J_1 = -(d_1/c) \cdot Y_d \cdot E_1 \end{array} \tag{12}$$

(a) Parameters Y_{ij} of the Attenuator

According to the matrix relation (8) and the relation (12) we can write:

$$\begin{cases} J_0 = Y_{11Cpl} \cdot E_0 + Y_{12Cpl} \cdot E_1 + Y_{13Cpl} \cdot E_2 \\ J_1 = Y_{21Cpl} \cdot E_0 + Y_{22Cpl} \cdot E_1 + Y_{23Cpl} \cdot E_2 = -(d_1/c) \cdot Y_d \cdot E_1 \\ J_2 = Y_{31Cpl} \cdot E_0 + Y_{32Cpl} \cdot E_1 + Y_{33Cpl} \cdot E_2 \end{cases} \tag{13}$$

From where the following relation:

$$\begin{cases} J_0 = Y_{11Att} \cdot E_0 + Y_{12Att} \cdot E_2 \\ J_2 = Y_{21Att} \cdot E_0 + Y_{22Att} \cdot E_2 \end{cases} \tag{14}$$

Whose expressions of the parameters Y_{ijAtt} of the attenuator are given in appendix.

(b) Parameters S_{ij} of the Attenuator

Parameters Y_{ijAtt} of the attenuator were found as well as the characteristic impedance Z_C. What enables us to deduce that the parameters S_{ij} from the attenuator for only at one point of operation of diode P.I.N (R_i = fixed) by:

$$S_{11Att} = \frac{(1 - Z_c \cdot Y_{11Att})(1 + Z_c \cdot Y_{22Att}) + Z_c^2 \cdot Y_{12Att} \cdot Y_{21Att}}{(1 + Z_c \cdot Y_{11Att})(1 + Z_c \cdot Y_{22Att}) - Z_c^2 \cdot Y_{12Att} \cdot Y_{21Att}} \tag{15}$$

$$S_{21Att} = \frac{-2 \cdot Z_c \cdot Y_{21Att}}{(1 + Z_c \cdot Y_{11Att})(1 + Z_c \cdot Y_{22Att}) - Z_c^2 \cdot Y_{12Att} \cdot Y_{21Att}} \tag{16}$$

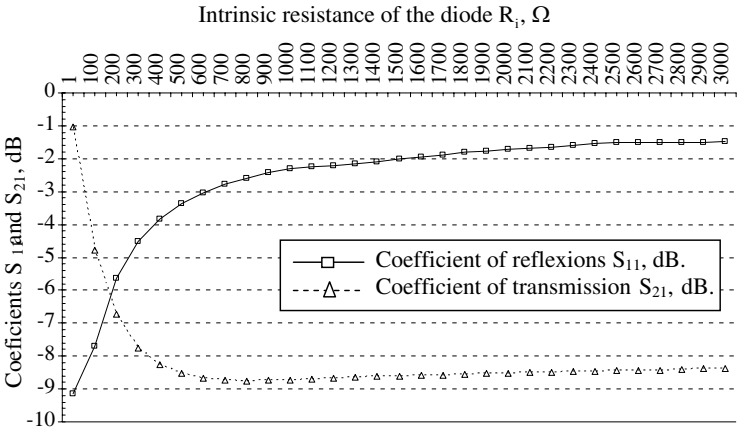

Figure 7. Variation of the coefficients of reflexions S_{11} and of transmission S_{21} according to R_i (for $f = 3\,\text{GHz}$).

3. RESULTS OF CARRIED OUT SIMULATIONS

In mode of direct polarization, the diode has a variable resistor whose value is inversely proportional to current I_d. According to the results presented at Figure 7, we deduce that if the equivalent resistance of the diode decreases, S_{11} decreases and S_{21} increases. The signal is less and less attenuated.

4. VALIDATION OF THE ANALYSIS METHOD

The validation of our method is ensured by confronting our results to those calculated by software ADS. The latter is based on the method of the moments. This method is very interesting since it is employed by the majority of the most important editors of electromagnetic simulators [9]. An evaluation of the number of fundamental operations in the iterative method (F.W.C.I.P) and the method of moments (ADS) was made in the reference [10]. It showed that starting from a certain density of grid of the study structure (Figure 8), the economy in a number of operations, therefore in computing times, is then considerable and widely justifies the use of the F.W.C.I.P. compared to the method of the moments. Moreover the iterative method is always convergent [10] and the absence of the functions of test facilitates its implementation, which allows a fast and total design of microwaves circuits to be realized.

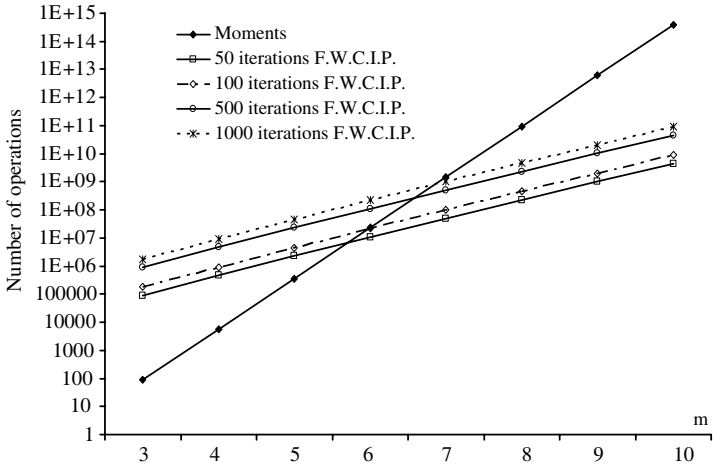

Figure 8. Comparison between the F.W.C.I.P. and the method of the moments ($K = 10$).

In the method of moments, the number of operations N_{Op_Mom} can be calculated using:

$$N_{Op\_Mom} = \frac{P^3}{3} = \frac{1}{3}\left(\frac{N}{K}\right)^3 \tag{17}$$

with P being the number of test functions.

$$K = \frac{\text{total surface}}{\text{metal surface}} = \frac{K \cdot P}{P} \tag{18}$$

$K \cdot P$: total number of pixels.

In the FWCIP method, the number of operations N_{op_FWCIP} performed in n iterations can be obtained from:

$$N_{Op\_FWCIP} = n \cdot (3N + 6N \log_e N) \tag{19}$$

n: is the iteration number necessary to the convergence of the results in the iterative method. N: is the number of modes TE and TM necessary to correctly describe the fields in the structure.

According to the theorem of Shannon, N is selected almost equal to $K \cdot P$:

$$N = K \cdot P \tag{20}$$

N is equal to a power of 2:

$$N = 2^{2m} \tag{21}$$

It is noted for example if $K = 10$, $m = 7$ (that is to say a structure with a grid by 128×128 pixels), the F.W.C.I.P is more interesting

than the method of the moments. $n = 500$ iterations constitutes the maximum ever observed for a good convergence.

The comparison between our results and those calculated by software ADS (Figure 9) shows that they have the same graphs and the minimal reflection is obtained with a frequency of $f = 7\,\text{GHz}$ with an error of 2.8%, for a length of the diode $d = 1.275\,\text{mm}$ ($d/\lambda g = 0.07$). The divergence between the two results can be reduced by furthermore decreasing the diode dimensions. If we increase the length of the diode $d = 7.45875\,\text{mm}$ ($d/\lambda g = 0.55$), the two graphs keep the same form but move away one from the other and the minimal reflexion is obtained with a frequency of $f = 8.4\,\text{GHz}$. Error increases at 19%.

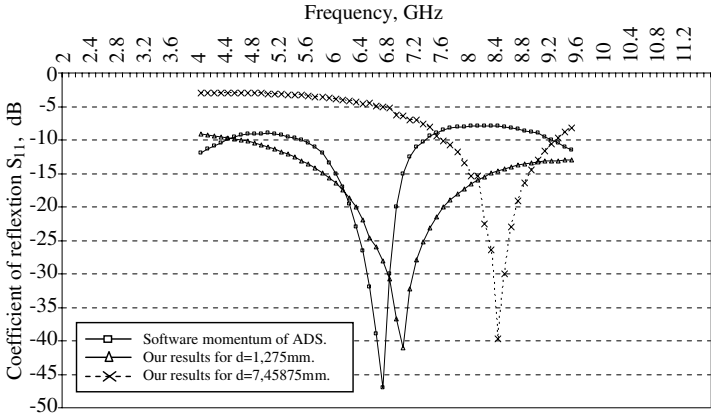

Figure 9. Variation of the coefficient of reflexion S_{11} in function of the frequency (for $R_i = 1\,\Omega$).

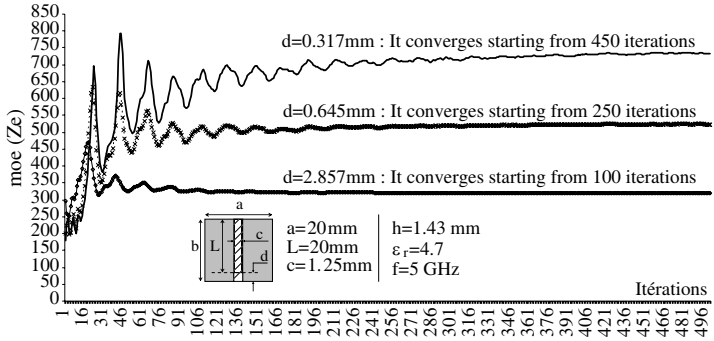

Figure 10. Divergent solutions due to the use of dot size excitation source in the iterative method.

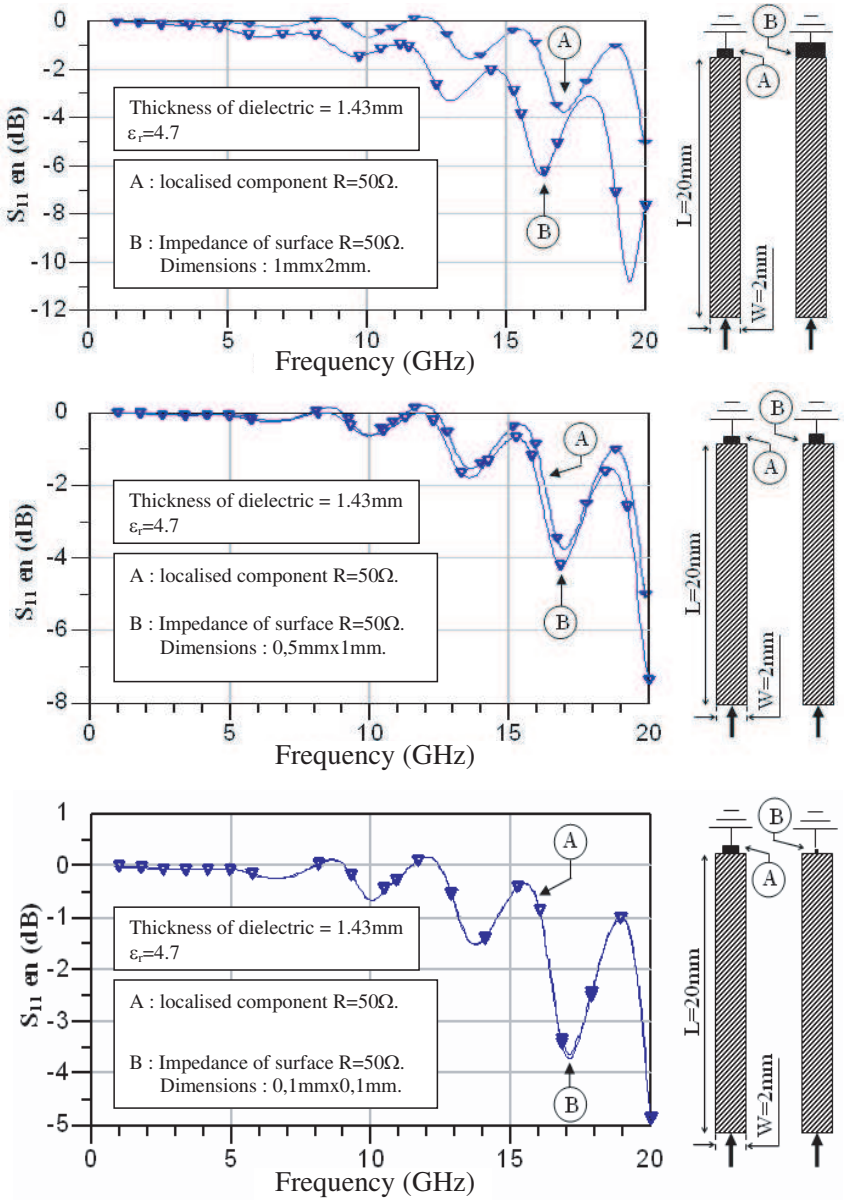

Figure 11. The divergence of the results due to the use of localised components having different sizes.

The difference between our results (for $d = 1.275\,\text{mm}$) and those calculated by software ADS can come from the use of localised components of different sizes. ADS uses the dot size localised components as Figure 3 confirms it. But in our model the localised component (diode) is planar, of defined dimensions and lower than the wavelength. It is replaced by an auxiliary source of excitation having the same dimensions as the latter, in order to be able to calculate the electromagnetic coupling between the various elements of the circuit. We avoid using dot size sources of excitations (therefore of the dot size components) since we are likely to have divergent solutions as shown in Figure 10 (this requires a considerable number of basic functions).

Figure 10 represents the convergence of the module of the impedance of entry of a microstrip line supplied by a planar source of variable size (cxd). These results confirm that the number of the iterations necessary to the convergence of the results increases with the reduction in the area occupied by the source of excitation. It is thus enough to introduce dot size sources, for discontinuities to appear and produce errors due to the divergences of the series.

Figure 11 represents the results of simulations under software ADS of two different structures (A and B). The first one (A) contains a microstrip line supplying a localised component (resistor of $50\,\Omega$) fixed size imposed by the software momentum of ADS. The second structure (B) contains a microstrip line supplying an impedance of surface of $50\,\Omega$ variable dimensions.

By observing the three graphs of Figure 11, we notice that the results of both structures coincide when dimensions of the impedance of surface decrease and approach of the dot size model. This confirms that the software momentum ADS uses dot size localised components which is not true in reality.

The use of different size localised components between our model and the software ADS can be a source of errors leading to the difference between the two results of simulations represented by Figure 9.

5. CONCLUSION

In this article, we highlighted the interest of a new method of calculation of the planar circuits integrating active elements (ultra high frequency diodes). This technique is based on the iterative method using localised auxiliary sources. Through this method we note the superiority of the use of the auxiliary sources by the simplicity of the formulation of the problem and by reducing the electromagnetic calculation of the studied structure. This calculation is made only once, for a passive or active, linear or no-linear component and

which can be changed without any influence on the final result. Nevertheless this technique can be validated only for low dimensions of these components, where the electromagnetic coupling between the latter and their environment remains weak. The comparison of the results shows a good agreement with those obtained by the software momentum of ADS.

APPENDIX A.

A.1. Space Field

The interface Ω (Figure 2) is made up various areas. On each area, the electromagnetic field checks the boundary conditions following:

$$\begin{cases} E_1' = E_2' = E_0 : \text{ on the excitation source area.} \\ \qquad\qquad\qquad\qquad (E_0 : \text{Electric field of the excitation source}) \\ E_1^{'} = E_2^{'} = E_1 : \text{ on the auxiliary source area.} \\ \qquad\qquad\qquad\qquad (E_1 : \text{Electric field of the auxiliary source}) \\ E_1^{'} = E_2' = 0 : \quad \text{on the metal area.} \\ E_1^{'} = E_2' \text{ and } J_1^{'} + J_2^{'} = 0 : \text{on the dielectric area.} \end{cases}$$

E_1' & E_2': Tangential electric fields on both sides of the Ω plan.

These conditions make it possible to express the operator of diffraction $\hat{\Gamma}_\Omega$, (the source of excitation is a source of electric field polarized according to oy) by:

$$\begin{bmatrix} \\ \hat{\Gamma}_{\Omega}\begin{bmatrix} x \\ y \end{bmatrix} \\ \\ \end{bmatrix} =$$

$$\begin{bmatrix} -\hat{H}_m - \left[\frac{1}{\frac{Z_{01}Z_{02}+Z_0(Z_{01}-Z_{02})}{Z_{01}Z_{02}+Z_0(Z_{01}+Z_{02})}}\right]\cdot\hat{H}_{Si} & \left[\frac{0}{\frac{2Z_0\sqrt{Z_{01}Z_{02}}}{Z_{01}Z_{02}+Z_0(Z_{01}+Z_{02})}}\right]\cdot\hat{H}_{Si} \\ +\frac{Z_{02}-Z_{01}}{Z_{01}+Z_{02}}\cdot\hat{H}_i & +\frac{2\sqrt{Z_{01}Z_{02}}}{Z_{01}+Z_{02}}\cdot\hat{H}_i \\ \left[\frac{0}{\frac{2Z_0\sqrt{Z_{01}Z_{02}}}{Z_{01}Z_{02}+Z_0(Z_{01}+Z_{02})}}\right]\cdot\hat{H}_{Si} & -\hat{H}_m - \left[\frac{1}{\frac{Z_{01}Z_{02}+Z_0(Z_{02}-Z_{01})}{Z_{01}Z_{02}+Z_0(Z_{01}+Z_{02})}}\right]\cdot\hat{H}_{Si} \\ +\frac{2\sqrt{Z_{01}Z_{02}}}{Z_{01}+Z_{02}}\cdot\hat{H}_i & -\frac{Z_{02}-Z_{01}}{Z_{01}+Z_{02}}\cdot\hat{H}_i \end{bmatrix}$$

with: Z_{01} and Z_{02} are the impedances of mediums 1 and 2. $Z_0 = (Z_{01}\cdot Z_{02})/(Z_{01}+Z_{02})$ is the internal impedance of the source.

To describe the interface Ω, we discreitize it in the form of pixels

and we introduce the operators H_m, H_i and H_{Si}, defined as follows:

$$H_m = \begin{cases} 1 & \text{on metal} \\ 0 & \text{elsewhere} \end{cases}, \quad H_i = \begin{cases} 1 & \text{on insulator} \\ 0 & \text{elsewhere} \end{cases},$$

$$H_{Si} = \begin{cases} 1 & \text{on the source } S_i \{E_i, J_i\} \\ 0 & \text{elsewhere} \end{cases}.$$

Dimensions of these operators depend on the density of grid of the circuit.

A.2. Spectral Field

The use of the FMT requires that the space and modal fields are discrete. In the space field this discretization is carried out by a grid in small rectangular areas (pixels) of the interface Ω. Electromagnetic value and the incidental and reflected waves are represented by matrices whose dimensions depend on the density of grid of this interface. The FMT makes it possible to define the amplitudes of the modes TE and TM in the spectral field.

On the higher and lower cap of the metal case, wave A_k undergoes a total reflection to generate a reflected wave B_k such as:

$$\begin{bmatrix} B_k^{TE} \\ B_k^{TM} \end{bmatrix} = \begin{bmatrix} \Gamma_k^{TE} & 0 \\ 0 & \Gamma_k^{TM} \end{bmatrix} \cdot \begin{bmatrix} A_k^{TE} \\ A_k^{TM} \end{bmatrix}$$

The electric field $E(x, y)$ is broken up on the basis of mode TE and TM of the case and it is given by the following expression:

$$E(x,y) = \sum_{m,n} e_{mn}^{TE} \left| f_{mn}^{TE}(x,y) \right\rangle + e_{mn}^{TM} \left| f_{mn}^{TM}(x,y) \right\rangle$$

With: $f_{mn}^{TE}(x, y)$ and $f_{mn}^{TM}(x, y)$ are functions modes of the case of the circuit to be studied (in our case it is a guide of rectangular wave) which constitute an orthonormated basis in the modal field.

The amplitudes of the modes TE and TM are expressed by:

$$\begin{cases} e_{mn}^{TE} = \left\langle f_{mn}^{TE}(x,y) \middle| E(x,y) \right\rangle \\ \quad = \left\langle f_{xmn}^{TE}(x,y) \middle| E_x(x,y) \right\rangle + \left\langle f_{ymn}^{TE}(x,y) \middle| E_y(x,y) \right\rangle \\ e_{mn}^{TM} = \left\langle f_{mn}^{TM}(x,y) \middle| E(x,y) \right\rangle \\ \quad = \left\langle f_{xmn}^{TM}(x,y) \middle| E_x(x,y) \right\rangle + \left\langle f_{ymn}^{TM}(x,y) \middle| E_y(x,y) \right\rangle \end{cases}$$

In our application, we have chosen an electric wall case whose functions of modes are expressed respectively by the following relations:

Modes TE :

$$\begin{cases} f_{xmn}^{TE}(x,y) = \frac{n}{b} \cdot \frac{1}{\sqrt{\left(\frac{m}{a}\right)^2+\left(\frac{n}{b}\right)^2}} \sqrt{\frac{2\sigma_{mn}}{ab}} \cdot \cos\left(\frac{m\Pi x}{a}\right) \cdot \sin\left(\frac{n\Pi y}{b}\right) \\ f_{ymn}^{TE}(x,y) = -\frac{m}{a} \cdot \frac{1}{\sqrt{\left(\frac{m}{a}\right)^2+\left(\frac{n}{b}\right)^2}} \sqrt{\frac{2\sigma_{mn}}{ab}} \cdot \sin\left(\frac{m\Pi x}{a}\right) \cdot \cos\left(\frac{n\Pi y}{b}\right) \end{cases}$$

Modes TM :

$$\begin{cases} f_{xmn}^{TM}(x,y) = \frac{m}{a} \cdot \frac{1}{\sqrt{\left(\frac{m}{a}\right)^2+\left(\frac{n}{b}\right)^2}} \sqrt{\frac{2\sigma_{mn}}{ab}} \cdot \cos\left(\frac{m\Pi x}{a}\right) \cdot \sin\left(\frac{n\Pi y}{b}\right) \\ f_{ymn}^{TM}(x,y) = \frac{n}{b} \cdot \frac{1}{\sqrt{\left(\frac{m}{a}\right)^2+\left(\frac{n}{b}\right)^2}} \sqrt{\frac{2\sigma_{mn}}{ab}} \cdot \sin\left(\frac{m\Pi x}{a}\right) \cdot \cos\left(\frac{n\Pi y}{b}\right) \end{cases}$$

$$\begin{cases} \sigma_{mn} = 2 \; si \; (m \text{ et } n) \neq 0 \\ \sigma_{mn} = 1 \; si \; (m \text{ ou } n) = 0 \end{cases}$$

m, n: indices of the modes TE and TM.

The plan Ω being divided into pixels, we can carry out the change of variables according to:

$$\begin{cases} (x/a) = (i/N_{01}) \\ (y/b) = (j/N_{02}) \end{cases}$$

"a" and "b" are respectively the width and the length of the case following "ox" and "oy". "N_{01}" and "N_{02}" are respectively the number of pixels according to "ox" and "oy".

What makes it possible to write:

$$\left\langle \cos\left(\frac{m\Pi x}{a}\right) \cdot \sin\left(\frac{n\Pi y}{b}\right) \middle| E_x(x,y) \right\rangle = \sum_{i=1}^{N_{01}} \sum_{j=1}^{N_{02}} E_x(i,j) \,.\, \cos\left(\frac{m\Pi i}{N_{01}}\right) \cdot \sin\left(\frac{n\Pi j}{N_{02}}\right)$$

$$\left\langle \sin\left(\frac{m\Pi x}{a}\right) \cdot \cos\left(\frac{n\Pi y}{b}\right) \middle| E_y(x,y) \right\rangle = \sum_{i=1}^{N_{01}} \sum_{j=1}^{N_{02}} E_y(i,j) \,.\, \sin\left(\frac{m\Pi i}{N_{01}}\right) \cdot \cos\left(\frac{n\Pi j}{N_{02}}\right)$$

The amplitudes of the modes TE and TM can be written as follows:

$$\begin{pmatrix} e_{mn}^{TE} \\ e_{mn}^{TM} \end{pmatrix} = \sqrt{\frac{\frac{2\sigma_{mn}}{ab}}{\left(\frac{m^2}{a^2}\right)+\left(\frac{n^2}{b^2}\right)}} \cdot \begin{bmatrix} \left(\frac{n}{b}\right) & \left(-\frac{m}{a}\right) \\ \left(\frac{m}{a}\right) & \left(\frac{n}{b}\right) \end{bmatrix} \cdot \begin{bmatrix} \sum_{i=1}^{N_{01}} \sum_{j=1}^{N_{02}} E_x(i,j) \cdot \cos\left(\frac{m\Pi i}{N_{01}}\right) \cdot \sin\left(\frac{n\Pi j}{N_{02}}\right) \\ \sum_{i=1}^{N_{01}} \sum_{j=1}^{N_{02}} E_y(i,j) \cdot \sin\left(\frac{m\Pi i}{N_{01}}\right) \cdot \cos\left(\frac{n\Pi j}{N_{02}}\right) \end{bmatrix}$$

The transform of Fourier as a cosinus and sinus is given by:

$$2D - FFT_{\cos\sin}\begin{pmatrix} E_x(i,j) \\ E_y(i,j) \end{pmatrix} = \begin{bmatrix} \sum_{i=1}^{N_{01}} \sum_{j=1}^{N_{02}} E_x(i,j) \cdot \cos\left(\frac{m\Pi i}{N_{01}}\right) \cdot \sin\left(\frac{n\Pi j}{N_{02}}\right) \\ \sum_{i=1}^{N_{01}} \sum_{j=1}^{N_{02}} E_y(i,j) \cdot \sin\left(\frac{m\Pi i}{N_{01}}\right) \cdot \cos\left(\frac{n\Pi j}{N_{02}}\right) \end{bmatrix}$$

The transform of Fourier in (FMT) mode:

$$\begin{pmatrix} e_{mn}^{TE} \\ e_{mn}^{TM} \end{pmatrix} = \sqrt{\frac{\frac{2\sigma_{mn}}{ab}}{\left(\frac{m^2}{a^2}\right)+\left(\frac{n^2}{b^2}\right)}} \cdot \begin{bmatrix} \left(\frac{n}{b}\right) & \left(-\frac{m}{a}\right) \\ \left(\frac{m}{a}\right) & \left(\frac{n}{b}\right) \end{bmatrix} \cdot 2D - FFT_{\cos\sin}\begin{pmatrix} E_x(i,j) \\ E_y(i,j) \end{pmatrix}$$

$$= \text{FMT} \begin{pmatrix} E_x(i,j) \\ E_y(i,j) \end{pmatrix}$$

A.3. Parameters Y_{ijAtt} of the Attenuator

According to the relations (13) and (14) we can draw the parameters Y_{ijAtt} from the attenuator as follows:

$$Y_{11Att} = Y_{11Cpl} - \frac{Y_{12Cpl} \cdot Y_{21Cpl}}{Y_d \cdot \left(\frac{d_1}{c}\right) + Y_{22Cpl}};\ Y_{12Att} = Y_{13Cpl} - \frac{Y_{12Cpl} \cdot Y_{23Cpl}}{Y_d \cdot \left(\frac{d_1}{c}\right) + Y_{22Cpl}}$$

$$Y_{21Att} = Y_{31Cpl} - \frac{Y_{32Cpl} \cdot Y_{21Cpl}}{Y_d \cdot \left(\frac{d_1}{c}\right) + Y_{22Cpl}};\ Y_{22Att} = Y_{33Cpl} - \frac{Y_{32Cpl} \cdot Y_{23Cpl}}{Y_d \cdot \left(\frac{d_1}{c}\right) + Y_{22Cpl}}$$

REFERENCES

1. Guillouard, K., M. F. Wong, V. F. Hanna, and J. Citerne, "A new global finite element analysis of microwave circuits including lumped elements," *1996 IEEE MTT-S Int. Microwave Symp. Dig.*, 355–358, Sans Francisco, CA, Jun. 1996.

2. Verdeyne, S., V. Madrangeas, D. Cros, M. Aubourg, and P. Guillon, "Design of microwave devices using the finite element method," *MTT Workshop WFFH, Global EM Simulators*, 50–69, Sans Francisco, Jun. 1996.
3. Imtiaz, S. M. S. and S. M. EL-Ghazaly, "Global modeling of millimeter-wave circuits: electromagnetic simulation of amplifiers," *IEEE Transactions on Microwave Theory and Techniques*, Vol. 45, No. 12, 2208–2216, Dec. 1997.
4. Larique, E., et al., "Application de la méthode des éléments finis à la modélisation de composants micro-ondes actifs," *MTT, Workshop, Chapitre IEEE-MTT-ED*, "Les Simulateurs globaux", la Rochelle 27-28 Mai 1998.
5. Baudrand, H. and R. S. N'gongo, "Applications of wave concept iterative procedure," *Microwave Theory & Tech.*, Vol. 1, 187–197, 1999.
6. N'gongo, R. S. and H. Baudrand, "A new approach for microstrip active antennas using modal F.F.T algorithm," *IEEE AP-S International Symposium Ind. USNC/URSI National Radio Science Meeting*, Orlando, USA, Jul. 11–16, 1999.
7. Ayari, M., T. Aguili, and H. Baudrand, "More effciency of Transverse Wave Approach (TWA) by applying Anisotropic Mesh Technique (AMT) for full-wave analysis of microwave planar structures," *Progress In Electromagnetics Research B*, Vol. 14, 383–405, 2009.
8. Ayari, M., T. Aguili, and H. Baudrand, "New version of TWA using two-dimensional non-uniform fast fourier mode transform (2d-nuffmt) for full-wave investigation of microwave integrated circuits," *Progress In Electromagnetics Research B*, Vol. 15, 375–400, 2009.
9. Gauthier, F., "Les outils de conception RF et hyperfréquences," Février 2004 n° 144 Electronique.
10. Fethi, M., "Modélisation électromagnétique des structures actives planaires par une méthode itérative avec sources auxiliaires localisées," Thèse de doctorat, E.N.I.T., Apr. 2006.